# UC Irvine
## UC Irvine Previously Published Works

**Title**

Toward improved identifiability of hydrologic model parameters: The information content of experimental data

**Permalink**

**Journal**

Water Resources Research, 38(12)

**ISSN**

0043-1397

**Authors**

Vrugt, Jasper A
Bouten, Willem
Gupta, Hoshin V
et al.

**Publication Date**

2002-12-01

**DOI**

10.1029/2001wr001118

**Copyright Information**

Peer reviewed

### Correction published 12 March 2003

# Toward improved identifiability of hydrologic model parameters: The information content of experimental data

Jasper A. Vrugt and Willem Bouten

Institute for Biodiversity and Ecosystem Dynamics, University of Amsterdam, Amsterdam, Netherlands

Hoshin V. Gupta and Soroosh Sorooshian

Department of Hydrology and Water Resources, University of Arizona, Tucson, Arizona, USA

[1]   We have developed a sequential optimization methodology, entitled the parameter identification method based on the localization of information (PIMLI) that increases information retrieval from the data by inferring the location and type of measurements that are most informative for the model parameters. The PIMLI approach merges the strengths of the generalized sensitivity analysis (GSA) method [*Spear and Hornberger*, 1980], the Bayesian recursive estimation (BARE) algorithm [*Thiemann et al.*, 2001], and the Metropolis algorithm [*Metropolis et al.*, 1953]. Three case studies with increasing complexity are used to illustrate the usefulness and applicability of the PIMLI methodology. The first two case studies consider the identification of soil hydraulic parameters using soil water retention data and a transient multistep outflow experiment (MSO), whereas the third study involves the calibration of a conceptual rainfall-runoff model.    *INDEX TERMS:* 1860 Hydrology: Runoff and streamflow; 1875 Hydrology: Unsaturated zone; *KEYWORDS:* parameter estimation, soil hydraulic properties, rainfall-runoff modeling, identification most informative measurements

**Citation:**   Vrugt, J. A., W. Bouten, H. V. Gupta, and S. Sorooshian, Toward improved identifiability of hydrologic model parameters: The information content of experimental data, *Water Resour. Res.*, *38*(12), 1312, doi:10.1029/2001WR001118, 2002.

## 1.   Introduction

[2] Hydrologic models often contain parameters that cannot be measured directly, but can only be meaningfully inferred by calibration to a historical record of input-output data. In its most elementary form, calibration is performed manually by visually inspecting the agreement between observations and model predictions [*Janssen and Heuberger*, 1995; *Boyle et al.*, 2000]. More sophisticated approaches express the agreement or misfit between model and measurements quantitatively in terms of misfit measures and use an optimization algorithm to minimize this measure. The definition of these misfits should reflect the intended use of the model and should concern the model quantities, which are deemed important [*Gupta et al.*, 1998]. The aim of these model calibration procedures is to reduce the uncertainty in the correct choice of the parameter values (parameter uncertainty) while simultaneously accounting for structural inadequacies in the model and uncertainties in the values of the measured input-output time series [*Thiemann et al.*, 2001]. However, because hydrological models will, by nature, only render an approximate description of reality and because the data used for calibration contain measurement errors, estimates of parameters and dependent variables from these models are generally error-prone. That is, in most cases, there is not a single point in the parameter space associated with good simulations; in

some cases, there may not even exist a well-defined region, in the sense of a compact region interior to the prior defined parameter space.

[3] One of the serious limitations of classical automated optimization strategies, such as population-evolution-based search strategies [*Brazil and Krajewski*, 1987; *Brazil*, 1988; *Wang*, 1991; *Duan et al.*, 1992; *Sorooshian et al.*, 1993], the GLUE procedure [*Beven and Binley*, 1992; *Freer et al.*, 1996], Monte Carlo membership procedure [*Keesman*, 1990; *van Straten and Keesman*, 1991], or the prediction uncertainty method [*Klepper et al.*, 1991], is that they do not provide information about which sets of measurements are most informative for specific model parameters. Currently, such expertise is usually acquired by an individual only through extensive hands-on training (manual calibration) and experience with a specific model. As a trivial example, when using a manual calibration approach in rainfall-runoff modeling, periods dominated by base flow are used to estimate the base flow recession rate parameter of the model. Clearly, increased information retrieval from the data about the type and location of the most informative measurements provides useful information for optimal experimental design or monitoring strategies. This serves as an attempt to obtain unique parameter estimates, being a prerequisite for finding pedotransfer functions [*Schaap et al.*, 1998; *Duan et al.*, 2001].

[4] The purpose of this paper is to develop a sequential optimization algorithm, entitled the parameter identification method based on the localization of information (PIMLI), to

increase information retrieval from the data. The PIMLI algorithm is a hybrid approach that merges the strengths of the generalized sensitivity analysis (GSA) method [*Spear and Hornberger*, 1980], the Bayesian inference scheme used in the Bayesian recursive estimation (BARE) algorithm [*Thiemann et al.*, 2001], and the sampling efficiency of the Metropolis algorithm [*Metropolis et al*, 1953] to select those sets of measurements that contain the most information for the identification of specific model parameters. As measurements with the highest information content for the various model parameters are recursively assimilated by the PIMLI algorithm, the uncertainty associated with the parameter estimates reduces.

[5] This paper is organized as follows. Section 2 presents a general outline of the GSA method, the BARE algorithm, and the Metropolis algorithm as foundations for the PIMLI algorithm. In section 3, three case studies are used to illustrate the usefulness and applicability of the PIMLI methodology. The first case study considers estimating hydraulic parameters in the soil water retention curve of *van Genuchten* [1980], whereas the second case considers a multistep transient outflow experiment. In this section, we are especially concerned with the influence of the experimental range of measurements on the identifiability of the soil hydraulic parameters. Moreover, we discuss the weaknesses of the current parametric models of soil hydraulic properties. Finally, the third case study involves the calibration of a conceptual rainfall-runoff model. Section 4 presents a summary of the material presented in this paper.

## 2. Model Calibration

[6] The fundamental problem with which we are concerned is to estimate parameter values and their uncertainty from observed hydrological data (inputs) using a specified mathematical model that simulates actual input-output relations. Given a model structure, the uncertainty in the parameter estimates can be reduced by successively assimilating measurement data. Traditional methods of calibration lump all of the differences between model predictions and measurements in a residual vector $E(\beta) = \{e(\beta)_1, \ldots, e(\beta)_n\}$, without explicitly recognizing differences in model sensitivity of the model parameters to the various measurements. The purpose of this paper is to explicate a methodology entitled PIMLI to increase information retrieval from the data by identifying subsets of data that contain most information on the specific model parameters.

[7] The object of much experimentation is to study the relationship between a response or output variable y subject to error and input variables. Following *Thiemann et al.* [2001], the model hydrologic $\eta$ can be written as

$$\hat{y} = \eta(\xi|\beta) + e \qquad (1)$$

where $\hat{y} = (\hat{y}_1, \hat{y}_2, \ldots, \hat{y}_n)$ is an n × 1 vector of model predictions, $\xi = (\xi_{11}, \xi_{12}, \ldots, \xi_{np})$ is an n × p matrix of input variables, $\beta = (\beta_1, \beta_2, \ldots, \beta_p)$ is the vector of p unknown parameters, and e is a vector of statistically independent errors with zero expectation and constant variance $\sigma^2$.

[8] The aim of model calibration procedures is to reduce the uncertainty in the parameter values $\beta$ while

simultaneously accounting for uncertainties in the measured input-output time series (data uncertainty) and uncertainties in the structural ability of the model, $\eta(\xi|\beta)$, to simulate the processes of interest (model uncertainty). We assume that the mathematical structure of the model is essentially predetermined and fixed. We begin by introducing a prior probability density distribution on the possible parameter sets and denoting this density p($\beta$). The purpose of the prior distribution is to quantify the initial uncertainty about the model parameters before any input-output data are collected. In order to avoid favoring any initial value, a uniform prior over the range of parameters may often seem reasonable [*Beven and Binley*, 1992].

### 2.1. Generalized Sensitivity Analyses as First Level in the PIMLI Algorithm

[9] The PIMLI procedure is schematically summarized in Figure 1. In view of the inevitably complicated nature of the hydrological model $\eta(\xi|\beta)$, it is evident that an explicit expression for the statistical distribution of the parameters is not possible. Instead, we use the power of Monte Carlo simulations to estimate measures of central tendency and dispersion for the various densities. For a prescribed number of Monte Carlo simulations $m$, we randomly sample a parameter set $\beta_j = (\beta_{11}, \beta_{12}, \ldots, \beta_{1p})$ from the prior probability distribution $\beta_j \leftarrow p(\beta)$ and generate the corresponding output $\hat{y}$. This results in an ensemble of $m$ models, each with structure $\eta(\xi|\beta)$ and with a parameter vector $\beta_j$, which is a random member of the distribution p($\beta$). The next step is to ascertain which elements of the parameter vector are able to mimic the important characteristics of the system being studied as reflected in the observations y. For this, a criterion function is needed (cf. 2.2) that classifies any $\beta_j$ for each single element of the vector y as being a "good" or "bad" simulation. The partitioning of the parameter space into "good" or productive and "bad" or nonproductive regions allows the application of a large variety of multivariate statistical analyses in exploring differences in the posterior distributions associated with good and bad simulations, or in exploring the structure induced into the joint distributions of parameters associated with good simulations. This part of the PIMLI algorithm is directly related to the GSA method [*Spear and Hornberger*, 1980; *Spear et al.*, 1994].

### 2.2. Second Level: The Bayesian Recursive Estimation Algorithm

[10] The PIMLI algorithm implements the Bayesian inference scheme (see section B of Figure 1), recently used in recursive mode in the BARE algorithm, as a criterion function to distinguish between "good" and "bad" simulations [*Thiemann et al.*, 2001]. The Bayesian framework for statistical inference is suited to such problems, because it allows for the use of probability distributions to quantify the uncertainty in the parameters. Moreover, as Bayesian estimators properly represent measurement errors, the confidence intervals of the parameters can be evaluated formally [*Hollenbeck and Jensen*, 1998]. Assuming that measurement errors are mutually independent, each having the exponential density distribution $E(\sigma, \gamma)$, the likelihood of
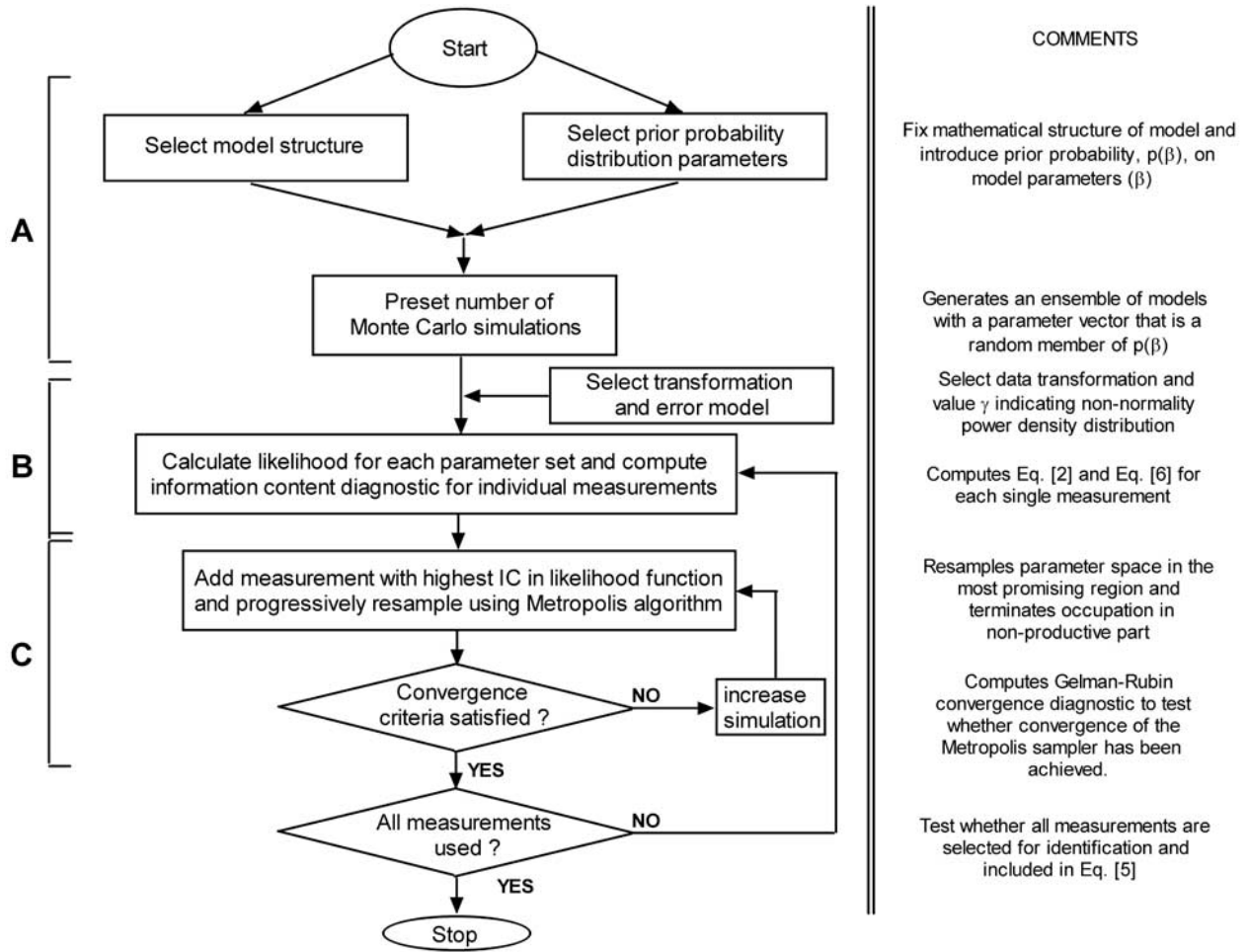
**Figure 1.** Schematic outline of the PIMLI algorithm combining the generalized sensitivity analyses (part A), Bayesian recursive estimation (part B), and Metropolis algorithm (part c).

parameter set $\beta_j$, $L(\beta_j, \sigma, \gamma | v_i)$ for describing $y_i$ can be calculated according to [*Box and Tiao*, 1973]

$$L(\beta_j, \sigma, \gamma | v_i) = \frac{w(\gamma)}{\sigma} \exp\left[-c(\gamma) \left|\frac{v_i}{\sigma}\right|^{\frac{2}{1+\gamma}}\right] \qquad (2)$$

where

$$v_i = g(\hat{y}_i) - g(y_i) \qquad (3)$$

and

$$c(\gamma) = \left\{\frac{\Gamma[3(1+\gamma)/2]}{\Gamma[(1+\gamma)/2]}\right\}^{\frac{1}{1+\gamma}}, \quad w(\gamma) = \frac{\{\Gamma[3(1+\gamma)/2]\}^{\frac{1}{2}}}{(1+\gamma)\{\Gamma[(1+\gamma)/2]\}^{\frac{3}{2}}} \qquad (4)$$

where y is the vector with observations, and $\gamma \in (-1,1]$ is a fixed "shape parameter" that can be regarded as a measure of kurtosis, indicating the extent of the nonnormality of the error density distribution. The density is normally distributed when $\gamma = 0$, double exponential when $\gamma = 1$, and tends to a uniform distribution as $\gamma \rightarrow -1$. The transformation $g(\cdot)$ in equation (3) allows us to handle heteroscedastic and

autocorrelated error cases in the residuals [e.g., *Sorooshian and Dracup*, 1980; *Kuczera*, 1988].

[11] The PIMLI algorithm proceeds by computing the posterior density for each single parameter set $\beta_j$ for each single measurement $y_i$

$$p(\beta_j, \sigma, \gamma | v_i) \propto L(\beta_j, \sigma, \gamma | v_i) p(\beta_j) \qquad (5)$$

According to equation (5) the "best" parameter set depends on the set of measurements, because $L(\beta_j, \sigma, \gamma | v_i)$ will always emphasize the ability of a certain parameter set to reproduce the selected observations. If a formerly superior parameter set, indicated by its prior density $p(\beta_j)$, cannot simulate the desired measurement $y_i$, it will receive lower weight in the computation of the posterior density, hence allowing a shift in the estimated elements of $\beta$. The posterior density, $p(\beta_j, \sigma, \gamma | v_i)$, associated with each parameter set $\beta_j$ is then sorted in ascending order and used to compute the cumulative distribution function. Based on an appropriate percentile (e.g., 95% interval), the model and classification criteria now provide a means of dividing the hypercube for each single measurement into two regions, one associated with "good" simulations and the other one with "bad". Finally, for the "good" simulations, the information content

(IC) of each successive observation for each member $\{\beta_{11}, \beta_{12}, \ldots, \beta_{1p}\}$ of parameter set $\beta_j$ is computed according to [see *Vrugt et al.*, 2001]

$$IC_{i,q} = 1 - \frac{\sigma_{\beta_{i,q}^{posterior}}}{\sigma_{\beta_{i,q}^{prior}}} \qquad i = 1 \ldots n, \ q = 1 \ldots p \qquad (6)$$

where $\sigma_{\beta_{i,q}^{prior}}$ and $\sigma_{\beta_{i,q}^{posterior}}$ denote the standard deviation of member q of parameter set $\beta_j$ in the prior and posterior probability distribution, respectively. If, for each successive member of $\beta_j$, the IC diagnostic is close to zero after processing measurement $y_i$, this implies a lack of information in that particular observation for identification purposes. In contrast, if one of the parameters in the "good" parameter sets occupies a single well-defined region internally of its prior distribution, measurement $y_i$ is informative for this parameter, thereby resulting in an IC value close to one.

### 2.3. Third Level: The Metropolis Algorithm for Assessing Parameter Uncertainty

[12] In the third step of the PIMLI procedure (part C of Figure 1), the measurement with the highest information content is added within a Metropolis sampling framework to progressively resample the parameter space in the most promising region, while relinquishing occupations in the nonproductive portions of the parameter space. This prevents the algorithm from collapsing to a single best parameter set by recursively assimilating more informative measurements, thus addressing a deficiency of BARE developed by *Thiemann et al.* [2001]. The Metropolis algorithm has received considerable attention in the last decade in the Bayesian statistics literature and is closely related to the probabilistic optimization technique called simulated annealing [*Metropolis et al.*, 1953; *Kirkpatrick et al.*, 1983].

[13] A Markov Chain Monte Carlo method for assessing parameter confidence intervals in nonlinear models is based on the idea that, rather than compute a probability density, $p(\beta)$, it is sufficient to have a large random sample from $p(\beta)$ that approximates the form of the density. Intuitively, if the sample were large enough, diagnostic statistical measures of the probability density function can be computed using the mean and standard deviation of the large sample. The most general and earliest MCMC algorithm, known as the Metropolis algorithm [*Metropolis et al*, 1953], is given as follows:

1. Randomly start at a location in the feasible parameter space, $\beta^{(t)} = \beta^{(0)}$, and compute the posterior density of this parameter set, $p(\beta^t|\mathbf{D})$, based on the set of measurements included in $\mathbf{D}$ using equations (2), (3), and (4).

2. Sample a new parameter set $\beta^{(t+1)}$ using the multinormal distribution as proposal distribution

$$\beta^{(t+1)} \leftarrow N\left(\beta^{(t)}, c^2 \Sigma_\beta\right) \qquad (7)$$

where $\beta^{(t)}$ is the mean, $\Sigma_\beta$ is the covariance matrix of $\beta$, and c is a scaling factor, typically in the range of $1-3$ to ensure that one can sample from regions of $p(\beta|\mathbf{D})$ which are not adequately approximated by the multinormal distribution in equation (7).

3. Calculate $p(\beta^{(t+1)}|\mathbf{D})$ and compute the ratio $\Omega = p(\beta^{(t+1)}|\mathbf{D})/p(\beta^{(t)}|\mathbf{D})$.

4. Randomly sample a uniform label Z over the interval 0 to 1.

5. If $Z \leq \Omega$, then accept the new configuration. However, if $Z > \Omega$, then remain at the current position, that is, $\beta^{(t+1)} = \beta^{(t)}$.

6. Increment $t$. If $t$ is less than a prespecified number of draws N, then return to step 2.

[14] The Metropolis algorithm will always accept candidate points (jumps) into a region of higher posterior probability, but will also explore regions with lower posterior probability with probability $\Omega$. This algorithm is a Markov Chain Monte Carlo sampler generating a sequence of parameter sets, $\{\beta^{(0)}, \beta^{(1)}, \ldots, \beta^{(t)}\}$, that converges to the stationary distribution, $p(\beta|\mathbf{D})$ for large n [*Gelman et al.*, 1997]. Thus, if the algorithm is run sufficiently long, the samples generated can be used to estimate statistical measures of the posterior distribution, such as mean, variance, etc. To speed up the convergence rate of the Metropolis sampler to the posterior target distribution, the covariance matrix of the proposal distribution, $\Sigma_\beta$, was periodically updated using a sample of the $\beta$s generated in the Markov Chain [*Kuczera and Parent*, 1998]. A heuristic strategy based on running $p$ multiple sequences generated in parallel was used to test whether convergence of the Metropolis sampler to a stationary posterior target distribution has been achieved [*Gelman and Rubin*, 1992]. Moreover, the initial proposal distribution in equation (7) was approximated using the mean value and covariance structure induced in the "good" parameter sets derived from level 2.

[15] After Metropolis sampling, the information content of the remaining $n - 1$ measurements is computed, using the Bayesian inference scheme. The PIMLI procedure continues until all observations are selected for identification purposes and included in $\mathbf{D}$. We would like to emphasize that the PIMLI algorithm presented here differs from our previous methodology [*Vrugt et al.*, 2001] in the sense that simply one objective function is used to simultaneously identify all of the parameters. During the course of our investigations, we became aware that the explicit presence of strong parameter interdependence and model errors significantly lowers the chance of finding disjunctive subsets of data each containing explicit information for just one of the model parameters.

### 3. Case Studies

[16] We illustrate the power and applicability of the PIMLI algorithm by means of three case studies. The first is a case study in which the four-parameter water retention function of *van Genuchten* [1980] is fitted to synthetic measurements. This illustrates the insights, which the PIMLI algorithm can offer with respect to parameter identifiability and optimal experimental design strategies. The second case study explores the utility of the PIMLI algorithm for identifying measurement sets that are most informative for the unsaturated soil hydraulic parameters, using a laboratory multistep outflow experiment. To explore the applicability of the PIMLI algorithm in the presence of measurement and model errors, the last case study involves the calibration of a conceptual rainfall-runoff model using hydrologic data from the Leaf River basin near Collins,

**Table 1.** Soil Hydraulic Parameters for the Sandy Soil and Their Initial Uncertainty (a priori Parameter Ranges) Used With the PIMLI Algorithm

| Parameter | Sand[a] | Min. | Max. | Unit |
|---|---|---|---|---|
| $\theta_s$ | 0.353 | 0.300 | 0.600 | [$m^3\ m^{-3}$] |
| $\theta_r$ | 0.033 | 0.000 | 0.300 | [$m^3\ m^{-3}$] |
| $\alpha$ | 2.122 | 0.100 | 5.000 | [$m^{-1}$] |
| n | 5.665 | 1.050 | 10.00 | |
| $K_s$ | 0.500 | 0.01 | 1.00 | [$m\ d^{-1}$] |
| l | 0.039 | −2.00 | 2.00 | |

[a] Adapted from *Vrugt and Bouten* [2001].

Mississippi. In all case studies, we assume a Gaussian error model (i.e., $\gamma = 0$) and a uniform prior distribution p($\beta$) for each of the parameters. Based on our previous work, the jump rate was fixed to 0.5 [*Vrugt and Bouten*, 2002].

### 3.1. Case Study I: Water Retention Model

[17] One of the most commonly used models of capillary pressure-saturation is the water retention function of *van Genuchten* [1980]

$$\theta(\psi) = \theta_r + (\theta_s - \theta_r)[1 + (\alpha|\psi|)^n]^{\frac{1}{n}-1} \qquad (8)$$

in which $\theta$ ($L^3\ L^{-3}$) denotes water content, $\theta_s$ and $\theta_r$ ($L^3\ L^{-3}$) are the water contents at full and residual saturation, respectively, $\psi$ (L) is the soil water pressure head, $\alpha$ ($L^{-1}$) is related to the inverse of the air-entry value, and n is a unitless pore size distribution index. Because, $\theta_s$, $\theta_r$, $\alpha$, and n are unknown model parameters, their values must be estimated through calibration.

[18] Synthetic ($\psi, \theta$) measurements were generated by using the parameters $\theta_s$, $\theta_r$, $\alpha$, and n given in Table 1 for a sandy soil and by evaluating equation (8) for a given set of pressure heads. For this, the logarithmic pressure head was discretized into 50 equidistant points between $\psi = -0.01$ and $\psi = -10^5$ m. Because the exact results are known, this set of water retention observations serves as a way of demonstrating the usefulness and applicability of the PIMLI algorithm. In addition, the synthetic "true" water content measurements were corrupted with error to investigate the effects of data error on the selection procedure. Data error may be regarded as representing the combined effects of measurement error and soil nonhomogeneity, which are not represented in the model. We assume here that this data error can be represented as a normally distributed N(0, $\sigma^2$) error term, which is added to the exact water contents [*Kool and Parker*, 1988]. The error standard deviation for water content is taken to be 0.005 ($L^3\ L^{-3}$). Figure 2 shows the original generated water content measurements as well as the effect of the data error on these synthetic water content measurements for the sandy soil in the range $0 \le pF \le 4$. The feasible parameter space for the parameters $\theta_s$, $\theta_r$, $\alpha$, and n was defined by the bounds given in Table 1. The results derived with the PIMLI algorithm for both the uncorrupted and corrupted error case are discussed below.

#### 3.1.1. Uncorrupted Water Retention Measurements

[19] In the case of no data error, the locations of the four most informative water content measurements identified and processed using the PIMLI algorithm, as being associated with each parameter, are indicated in Figure 3a. The sequen-
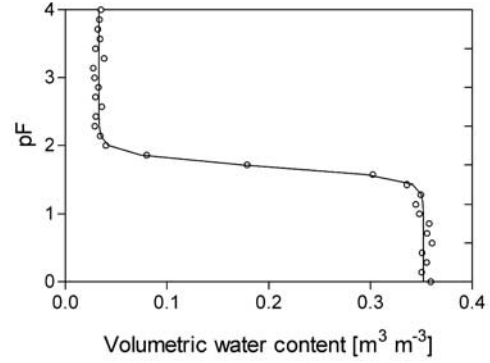


**Figure 2.** Water retention curve of the sandy soil and the effect of data error.

tial order in which the measurements are recursively identified and assimilated with the algorithm is indicated in the graph. Additionally, Figure 3b illustrates the general behavior of parameter sensitivity for the sandy soil in the VG model.
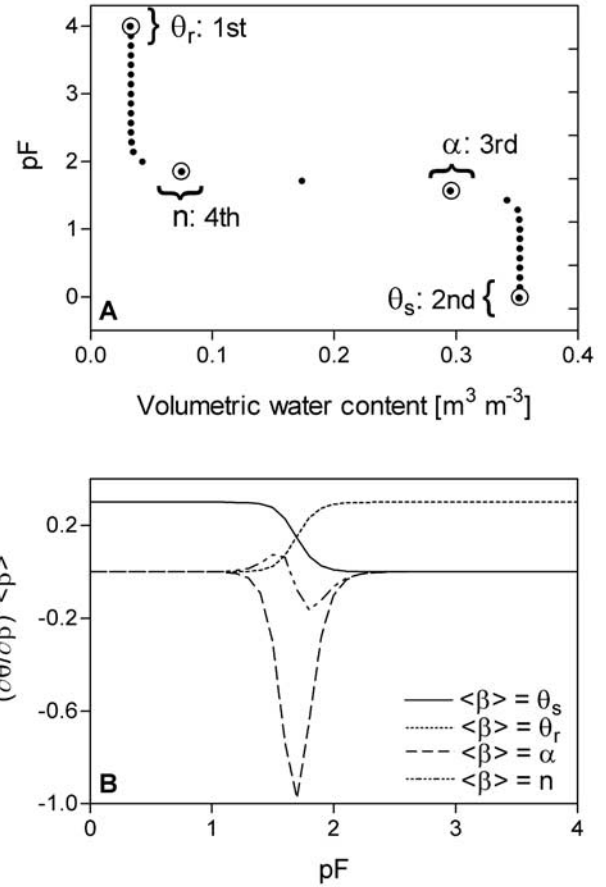


**Figure 3.** (a) Uncorrupted error case: location of the four most informative water retention measurements along the curve identified using the PIMLI algorithm. The sequential order in which the measurements are assimilated and processed is indicated with decreasing size of the white dots. (b) Behavior of sensitivity of water content to the water retention parameters $\theta_s$, $\theta_r$, $\alpha$, and n over the prior defined range of pressure head values for the sandy soil in the VG model.
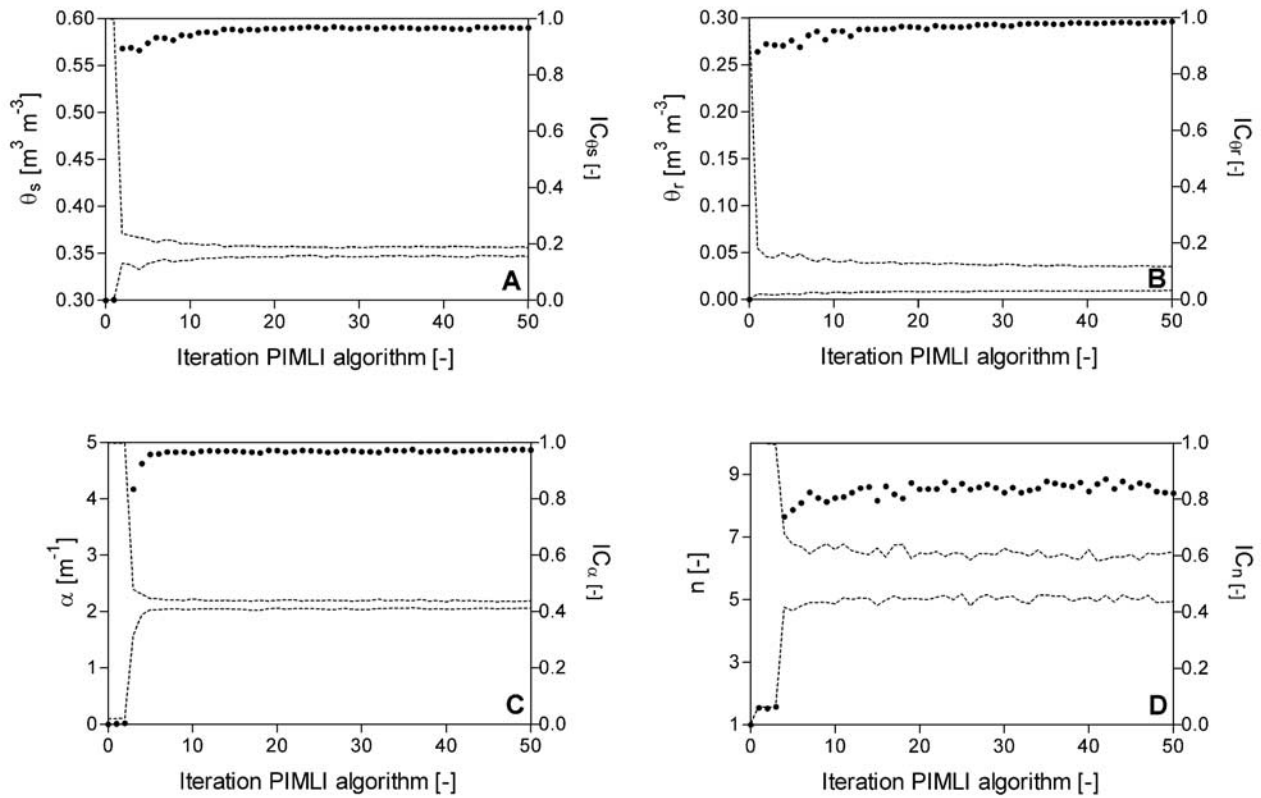
**Figure 4.** Evolution of the Bayesian confidence intervals and information content diagnostic of the VG retention parameters (a) $\theta_s$, (b) $\theta_r$, (c) $\alpha$, and (d) n for the sandy soil.

To allow comparison of sensitivity coefficients between different parameters, the Jacobian elements were scaled to the parameter's prior uncertainty ranges defined in Table 1.

[20] Moving from full to residual saturation, Figure 3a demonstrates that the most informative water content measurements are first found for $\theta_s$ close to saturation, then for $\alpha$ close to the air-entry value of the soil, for n at the inflection point in the low water content range, and finally for $\theta_r$ close in the low water content range, respectively. The location of these most informative measurements matches very well with the general behavior of parameter sensitivity, as illustrated in Figure 3b. Seemingly, some small deviations are found between the exact location of the most informative measurements along the curve, depicted in Figure 3a, and judgments about these locations based on the marginal sensitivity coefficients only. For instance, the PIMLI algorithm identifies a moisture content measurements at pF = 1.5 as most informative for the parameter $\alpha$, whereas Figure 3b suggests that the sensitivity to this parameter is larger for moisture content measurements at pF = 1.75. This discrepancy is attributed to parameter interdependence, as closer inspection of Figure 3b demonstrates that, at pF = 1.5, the overall sensitivity of the VG model to $\alpha$, being $|\partial\theta/\partial\alpha| - |\partial\theta/\partial n|$ is at its maximum.

[21] Besides the exact location of most informative measurements, the hierarchical selection order of the measurements is also strongly determined by the interdependency among the retention parameters. For instance, using the first-order sensitivity coefficients, it is expected that the PIMLI algorithm will first identify measurements close to pF = 1.75 as most informative for the parameter $\alpha$ because

the absolute magnitude of the sensitivity coefficients is largest at this pressure head and associated with the retention parameter $\alpha$. Again, the explicit presence of parameter interdependence in the range of pF = 1−3 increases the extent of the uncertainty associated with the parameter $\alpha$. Consequently, because volumetric water content measurements close to saturation (pF $\leq$ 1) and in the low water content range (pF $\geq$ 2.5) are almost solely sensitive to either the saturated or residual water content, these measurements are first selected to constrain the saturated and residual water content in the sampling. Once the first two measurements are successively assimilated and the uncertainty associated with the parameters $\theta_s$ and $\theta_r$ diminishes, the information for the retention parameters $\alpha$ and n appears from the water content measurements in the intermediate water content ranges.

[22] In Figure 4 we present the relative size of the high probability density (HPD) region, including the information content diagnostic for each of the retention parameters as functions of the number of water content measurements used for identification purposes. Because only one measurement is recursively added in the likelihood function (equation (2)) at a time, the value of the iteration number is equivalent to the number of measurements used for parameter identification. Figure 4 demonstrates that, as more and more measurements are assimilated with the PIMLI algorithm, the HPD region tends to concentrate on the most likely parameter values. Note, however, that the size of the HPD region will remain of finite size because we included the predefined water content data error term in equation (2). When processed efficiently, only a relatively small amount

of measurements are needed for a reliable identification for each of the model parameters. The PIMLI algorithm pinpoints the true parameter values for the perfect data case after processing approximately five water content measurements. Clearly, there is only a marginal improvement in the size of the 95% Bayesian confidence interval, centered on the "most likely" parameter set, between using the five most informative measurements and all 50 measurements. Seemingly, approximately 90% of the data contains information that is largely redundant for parameter identification purposes. It is not the "amount" of data that discriminates between parameter sets, but the information content of the data and the efficiency with which that information is extracted during model calibration [e.g., *Kuczera*, 1982; *Sorooshian et al.*, 1983; *Gupta and Sorooshian*, 1985]. The reason for the jumping behavior of the confidence limits for the parameter n, shown in Figure 4d, is that, to maintain computational efficiency, the Metropolis sampler was not allowed to densely resample the parameter space. Consequently, the exact Bayesian confidence limits are, to a certain extent, subject to the stochastic properties of the Metropolis sampler.

[23] The results presented in this case study illustrate two important findings. The first is that the newly developed sequential optimization methodology correctly infers the location and hierarchical selection order of the most informative measurements, without having a priori knowledge of the system properties (i.e., most optimal parameter set). The latter is a necessity to be able to draw these conclusions utilizing the first-order approximation. Another finding is that, in the case of perfect data, only a very limited amount of water content measurements is needed for a reliable estimation of the retention parameters.

### 3.1.2. Corrupted Water Retention Measurements and Experimental Design

[24] A more realistic case study is one in which the water retention observations are corrupted with data error. For this case, the four most informative water content measurements, identified using the PIMLI algorithm as being associated with each parameter, are indicated in Figure 5a. For illustrative purposes, we have temporarily switched the x and y axes of the retention characteristic. The striking resemblance between the Figures 3 and 5a demonstrates that the PIMLI algorithm is able to successfully infer the location of the most informative water content measurements in the presence of data error. Although not shown here, the data error resulted in slower convergence of the HPD region into the vicinity of the true parameter values used to generate the synthetic observations of the sandy soil in the forward mode. The Bayesian confidence intervals of the parameters reached a constant width after processing eight water content measurements.

[25] To further investigate the influence of the experimental range of pressure heads on the final uncertainty of the retention parameters, we performed the following experiment. Starting at $\psi = -10^5$ m (location I in Figure 5), two subsequent retention observations were omitted at each step from the original set of corrupted water content measurements, resulting in 25 data sets with varying numbers of observations {50, 48, 46,..., 2} thereby, varying experimental pressure head range before arriving at full saturation. These data sets were used as input for the PIMLI
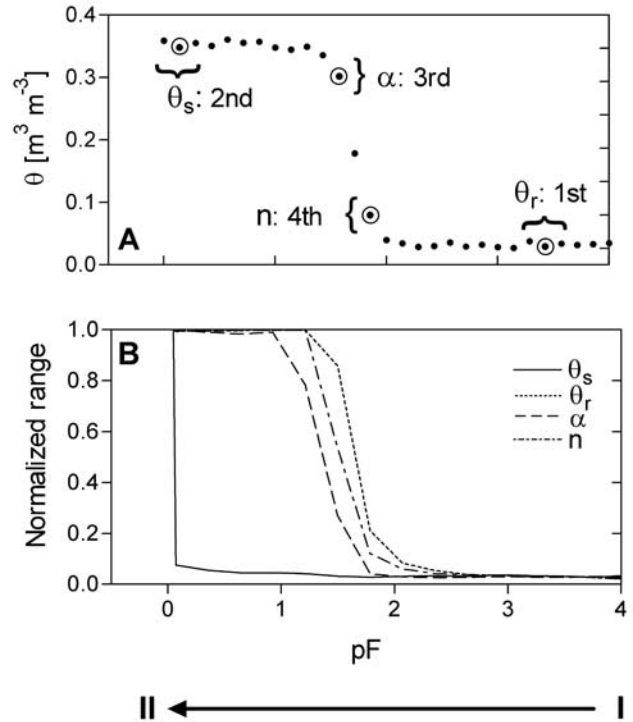


**Figure 5.** (a) Corrupted error case: location of the four most informative water retention measurements along the curve identified using the PIMLI algorithm. The sequential order in which the measurements are assimilated and processed is indicated with decreasing size of the white dots. (b) Normalized range of each of the retention parameters as function of the experimental range of pressure heads. For more explanation, see text.

algorithm to assess the corresponding uncertainty of the retention parameters. Figure 5a illustrates how the size of the HPD region for each of the parameters depends on the experimental range of pressure heads. To allow comparison between uncertainties of different parameters, the HPD region was scaled according to the prior uncertainty bounds of the parameters, defined in Table 1 to yield normalized ranges between 0 and 1. Omitting retention measurements in the dry water content range between $-10^2 \leq \psi$ [m] $\leq -10^0$ does not significantly affect the size of the confidence intervals of the parameters. Thereafter, the uncertainty associated with the parameters increases, reflecting the fact that the information for the parameters $\theta_r$, n, and $\alpha$ (in following order) is then starting to appear outside of the experimental range of pressure heads. Notice the striking resemblance in the shape of uncertainty curves depicted in Figure 5b and the functional shape of the water retention characteristic. Finally, when arriving at full saturation, the saturated water content remains well identifiable, while the normalized ranges of the other parameters then reflect their prior uncertainty bounds. This indicates the lack of information in retention measurements close to saturation for the residual water content and curve shape parameters $\alpha$ and n. In the interest of brevity, we have only presented graphical results for the sandy soil. For more fine-textured soils, the curves depicted in Figure 5a exhibit a more sigmoid shape reflecting the shape of the water retention characteristics for

those kinds of soils. In addition, with increasing water-holding capacity of the soils, the different curves shifted toward lower pressure head values.

[26] The results presented here illustrate that the PIMLI algorithm provides valuable information about the location and hierarchical selection order of the most informative measurements and can also be used to evaluate different experimental design strategies for their suitability for identifying the hydraulic parameters. The method therefore supports the identification of unique parameter values (preferably having a small variance) as a prerequisite for finding pedotransfer functions.

### 3.2. Case Study II: Synthetic Multistep Outflow Experiment

[27] A more demanding test of the PIMLI algorithm was devised by applying the algorithm to a synthetic, laboratory MultiStep Outflow experiment. The two basic soil hydraulic characteristics controlling flow in unsaturated porous media are the retention characteristic, $\theta(\psi)$ in equation (8), and the unsaturated hydraulic conductivity characteristic, $K(\psi)$

$$K(\psi) = K_s \frac{\left[1 - (\alpha|\psi|)^{n-1}(1 + (\alpha|\psi|)^n)^{\frac{1}{n}-1}\right]^2}{\left[1 + (\alpha|\psi|)^n\right]^{l\left(1-\frac{1}{n}\right)}} \qquad (9)$$

where $K_s$ is the saturated hydraulic conductivity $(LT^{-1})$, and $l$ (dimensionless) is an additional parameter related to the exponent parameter of *Mualem* [1976]. Because direct methods for determination of the $\theta(\psi)$ and $K(\psi)$ curve require rather restrictive initial and boundary conditions and are therefore relatively tedious, numerical inversion is an attractive alternative for determining both curves from a single experiment. In such an approach, the optimal soil hydraulic parameters are found by fitting a numerical solution of Richards' equation to observations of measured variables during the experiment. When a joint parametric description of retention and unsaturated hydraulic conductivity is assumed, inversion of the Richards equation will yield parameter estimates that apply to both characteristics simultaneously.

[28] Synthetic outflow measurements were generated for a soil core with a height of 5 cm. In keeping up with the previous case study, hydraulic properties were used that correspond to the sandy soil previously defined in Table 1. The HYDRUS-1D software package [*Šimůnek et al.*, 1998a] was used to numerically solve Richards' equation in one dimension using a Galerkin-type linear finite element scheme. As the initial condition, hydraulic equilibrium was assumed with a pressure head $\psi = -0.01$ m at the bottom of the soil core, and $\psi = -0.06$ m at the top. The following pressure head steps and time periods (in brackets) were applied in the numerical experiment, $\psi_1 = -0.0030$ m (0 $\leq 0.50$ d), $\psi_2 = -0.15$ m (0.50 $\leq 1.50$ d), $\psi_3 = -0.50$ m (1.50 $\leq 3.50$ d), $\psi_4 = -1.00$ m (3.50 $\leq 5.50$), $\psi_5 = -3.00$ m (5.50 $\leq 12.50$ d), and $\psi_6 = -5.00$ m (12.50 $\leq 20.00$ d). Subsequently, the unsaturated hydraulic properties were inversely estimated using the PIMLI algorithm in combination with the HYDRUS-1D code. The soil hydraulic parameters $\theta_s$, $\theta_r$, $\alpha$, n, $K_s$, and l were assumed to be unknown and having the prior uncertainty ranges defined in Table 1.

[29] Based on our earlier work [*Vrugt et al.*, 2001], we treated measured cumulative outflow, its first derivate (flux density), and the average water content in the soil core, deduced from observed cumulative outflow dynamics and the water content at the beginning of the experiment, as three separate measurement sets. The measurement error of the outflow was set to 0.05 cm³, which is identical to the accuracy of pressure transducers that are used for automated monitoring of the outflow dynamics in the laboratory. Subsequently, the measurement errors of the water content and flux density data sets were derived according to [*Vrugt et al.*, 2001] assuming an error in initial soil water content of 0.01 [m³ m⁻³]. The results obtained with the PIMLI algorithm using the synthetic outflow observations are discussed below.

[30] Moving from full to residual saturation during the outflow experiment, the location of the six most informative outflow observations for the various model parameters within the different "artificial" measurement sets is illustrated in Figure 6. The sequential selection order in which the measurements are recursively identified and assimilated with the PIMLI algorithm is indicated in the graph. Figure 6 illustrates that water content measurements at hydraulic equilibrium close to saturation are most informative for the saturated water content and therefore included in equation (5) to identify $\theta_s$. Additionally, cumulative outflow measurements at hydraulic equilibrium close to the air-entry value of the soil in the intermediate water content ranges and close to residual saturation are most informative for the curve shape parameters $\alpha$ and n and the residual water content, respectively. Finally, flux density measurements immediately after passing the air-entry value of the soil are most informative for the saturated hydraulic conductivity. No informative measurements in this experiment can be found for the pore connectivity parameter l because the information content diagnostic for this parameter exhibits relatively low values, implying a lack of information. Instead, measurements close to saturation, being associated with $\theta_s$, are recursively assimilated and processed with the PIMLI algorithm.

[31] There is a striking similarity in the location and hierarchical selection order of the most informative measurements for the parameters $\theta_s$, $\theta_r$, $\alpha$, and n found under transient conditions and similar results presented for the static retention characteristic (case study 1). In both cases, the most informative measurements for the saturated and residual water content are found at hydraulic equilibrium close to full and residual saturation, respectively. Additionally, the most information for $\alpha$ and n is located during hydraulic equilibrium conditions close to the air-entry value of the soil and in the intermediate water content range, respectively. Seemingly, the joint appearance of the parameter n in the retention and unsaturated soil hydraulic characteristic hardly affects the location of the most informative measurements being associated with this parameter during transient conditions.

[32] Although not presented for this case study, the evolution of the Bayesian confidence intervals of the parameters demonstrated that the PIMLI algorithm was able to exactly pinpoint the parameter values of the sandy soil used to generate the synthetic measurements after processing only 15 outflow measurements. There was only a marginal improvement in the size of the confidence intervals between using the 15 most informative measurements
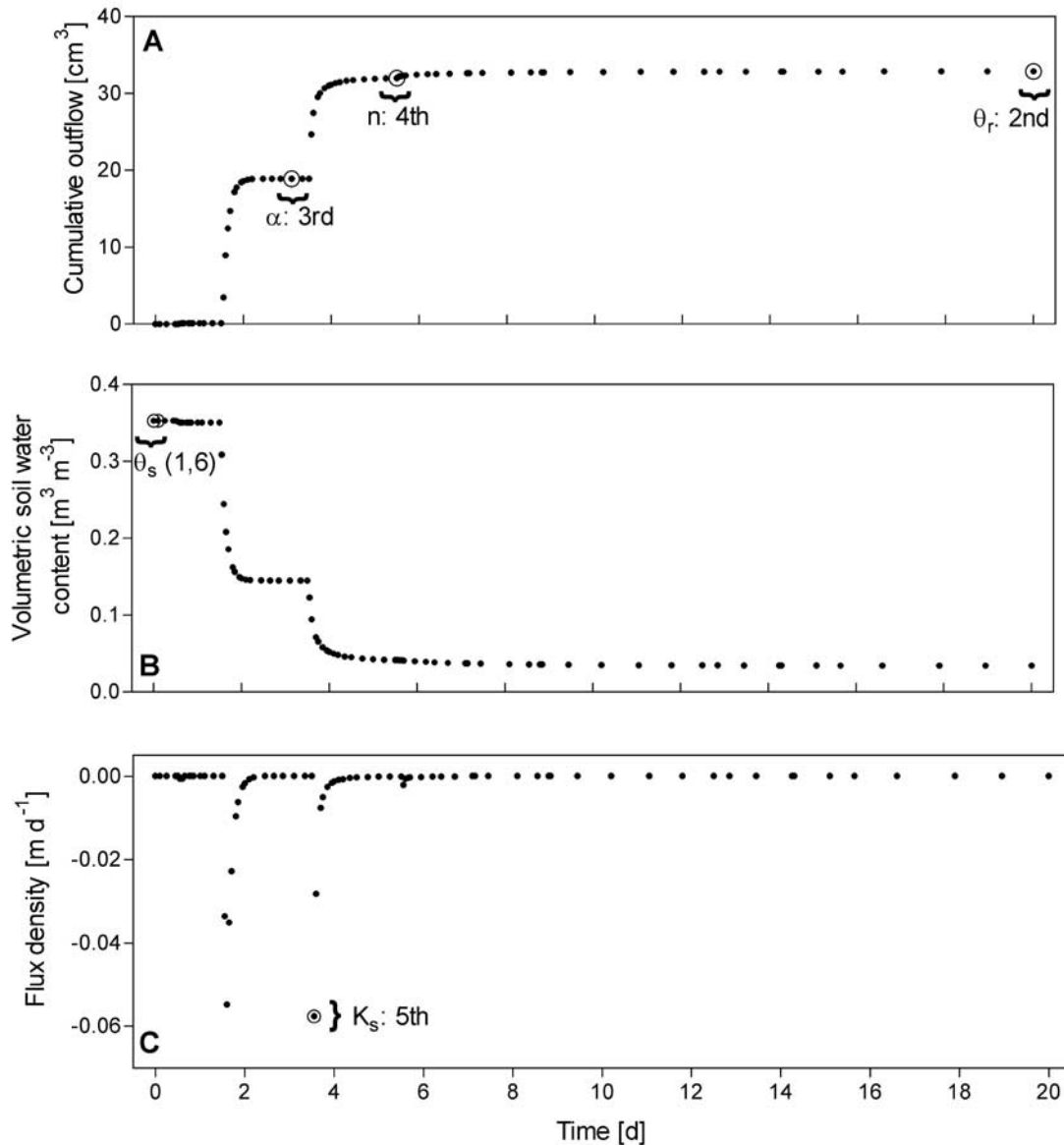
**Figure 6.** Synthetic outflow experiment: location of the six most informative outflow observations for the various model parameters within the different measurement sets. The sequential selection order in which the measurements are recursively identified and assimilated with the PIMLI algorithm is indicated with decreasing size of the circles.

and 225 synthetic measurements. Also under transient conditions, approximately 95% of the "synthetic" measurements contained redundant information for parameter identification purposes.

### 3.3. Discussion

[33] An important finding, illustrated by Figures 3, 5, and 6, is that for more fine-textured soils, problems occur with the simultaneous identification of the parameters $\theta_r$ and n, because conventional laboratory experiments generally yield a pressure head range between 0.1 and 10 m (1 < pF < 3). Unless augmented with laboratory measurements at relatively low water contents, the most informative measurements for the parameters $\theta_r$ and n are then beyond the experimental range, and estimation of these parameters is then based primarily on extrapolation. This leads to high correlation between estimates of $\theta_r$ and n, which is often

graphically found in response surfaces. Consequently, the inverse problem is ill-posed, especially in the case of measurement and model errors. There have been numerous reports in the literature of problems with the identification of the parameters $\theta_r$ and n on the basis of water content or pressure head data [see, e.g., *van Genuchten*, 1980; *Parker et al.*, 1985; *Šimůnek et al.*, 1998b; *Vrugt et al.*, 2001]. To avoid identifiability problems for $\theta_r$ and n, it is important to have some independent data or procedure for estimating the residual water content.

[34] Although the inclusion of a residual water content in the description of a water retention curve is physically correct [*Brooks and Corey*, 1964; *van Genuchten*, 1980; *Kosugi*, 1996], its value is controversial [*Luckner et al.*, 1989] and not supported by experimental data [*Rossi and Nimmo*, 1994] and its value is ill-determined from a inverse point of view as the most informative measurements for this
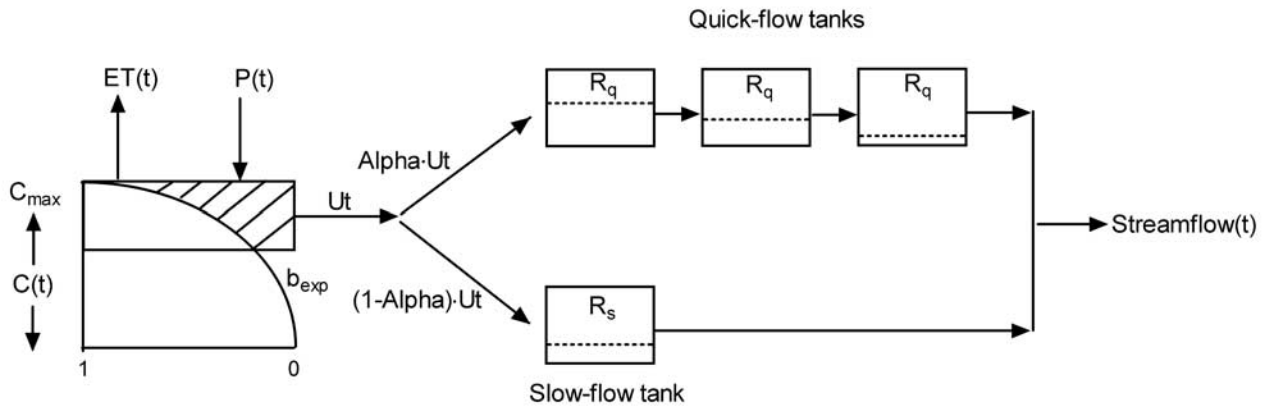
Quick-flow tanks



**Figure 7.** Schematic outline of the HYMOD conceptual watershed model.

parameter are, for most soils, usually far outside the measurement range. If in such cases $\theta_r$ is treated as an unknown parameter it strongly enhances the likelihood of nonuniqueness in the inverse problem. Lack of data at the dry end will, in any case, cause the optimized value of $\theta_r$ to be that of a fitting parameter without any physical significance [*Vereecken et al.*, 1997]. Identifiability problems for $\theta_r$ can be eliminated if one would independently measure $\theta_r$, or if one would use a water retention model, which does not explicitly contain a residual water content in the model formulation [*Rossi and Nimmo*, 1994]. This is an attractive alternative, as its suitability for characterizing the $\theta(\psi)$ and $K(\psi)$ curves is acceptable [*Rossi and Nimmo*, 1994], as compared to the models which explicitly contain $\theta_r$ in their model formulation [e.g., *Brooks and Corey*, 1964; *van Genuchten*, 1980; *Russo*, 1988; *Kosugi*, 1996].

### 3.4. Case Study III: Application to Conceptual Rainfall-Runoff Model

[35] The third study presented in this paper explores the usefulness of the PIMLI algorithm to the identification of parameters in a conceptual rainfall-runoff (CRR) model. The illustrative study here involves calibration of the HYMOD conceptual watershed model using approximately 1 year of historical data (28 July 1952 to 30 September 1953) from the Leaf River watershed near Collins, Mississippi. The HYMOD model (see Figure 7), first introduced by *Boyle* [2001], consists of a relatively simple rainfall excess model, described in detail by *Moore* [1985], connected with two series of linear reservoirs (three identical quick and a single reservoir for the slow response) and requires the optimization of five parameters to observed streamflow data: the maximum storage capacity in the catchment, $C_{max}$ [L], the degree of spatial variability of the soil moisture capacity within the catchment, $b_{exp}$ (dimensionless), the factor distributing the flow between the two series of reservoirs, Alpha (dimensionless), and the residence time of the linear quick and slow reservoirs, $R_q$ [T] and $R_s$ [T], respectively. Because the HYMOD model and Leaf River data have been discussed extensively in previous work [*Sorooshian et al.*, 1993; *Duan et al.*, 1993, 1994; *Boyle*, 2000; *Wagener et al.*, 2001], the details will not be presented here.

[36] To investigate whether the location of the most informative streamflow measurements in the hydrograph

is influenced by the presence of errors (measurement and model) in the observed hydrological data two experiments were performed. In the first experiment, the PIMLI algorithm was applied to synthetic daily streamflow data (in $m^3$/s), generated for the period 28 July 1952 to 30 September 1953, by driving HYMOD with mean areal boundary conditions for the selected 1-year period (rainfall and potential evapotranspiration) and fixed values for the parameters. The parameter values were set identical to their most optimal value derived when separately fitting the HYMOD model to the observed streamflows for the selected period using the SCE-UA global optimization algorithm [*Duan et al.*, 1992, 1993] and the RMSE criterion. In the second experiment the PIMLI algorithm was applied to the observed streamflows of the Leaf River watershed for the approximately one-year period under consideration. In both experiments, the measurement error of the streamflow data was fixed to the RMSE value of the most optimal parameter set obtained using the SCE-UA global optimization algorithm. Further, it was assumed that the output errors have a heteroscedastic variance that is related to flow level and which can be stabilized by the Box-Cox transformation using $\lambda = 0.3$ [e.g., *Sorooshian and Dracup*, 1980; *Thiemann et al.*, 2001]. To reduce sensitivity to state value initialization, a 65-day warm-up period was used during which no updating of the posterior density functions was performed. The results for each of the experiments are illustrated in Figure 8 and discussed below.

[37] Figures 8a presents the synthetic streamflow observations in the transformed space, while Figure 8b shows the lumped dynamics of soil-moisture storage within the watershed corresponding to the true parameter set for a portion of WY 1952. The open circles correspond to the location of the most informative streamflow measurements, whereas the number between parentheses refers to the hierarchical selection order. The results presented in the Figures 8a and 8b illustrate that the most informative streamflow measurements for the parameters $R_s$ and $R_q$ are located after the cessation of rainfall in the nondriven quick and nondriven slow parts of the hydrograph, respectively. Closer inspection of the information content diagnostic for these parameters demonstrated that the information for these parameters is typically independent of the storage in the slow, quick, and soil-moisture tank. On the contrary, Figure 8b demonstrates that the location of the most informative
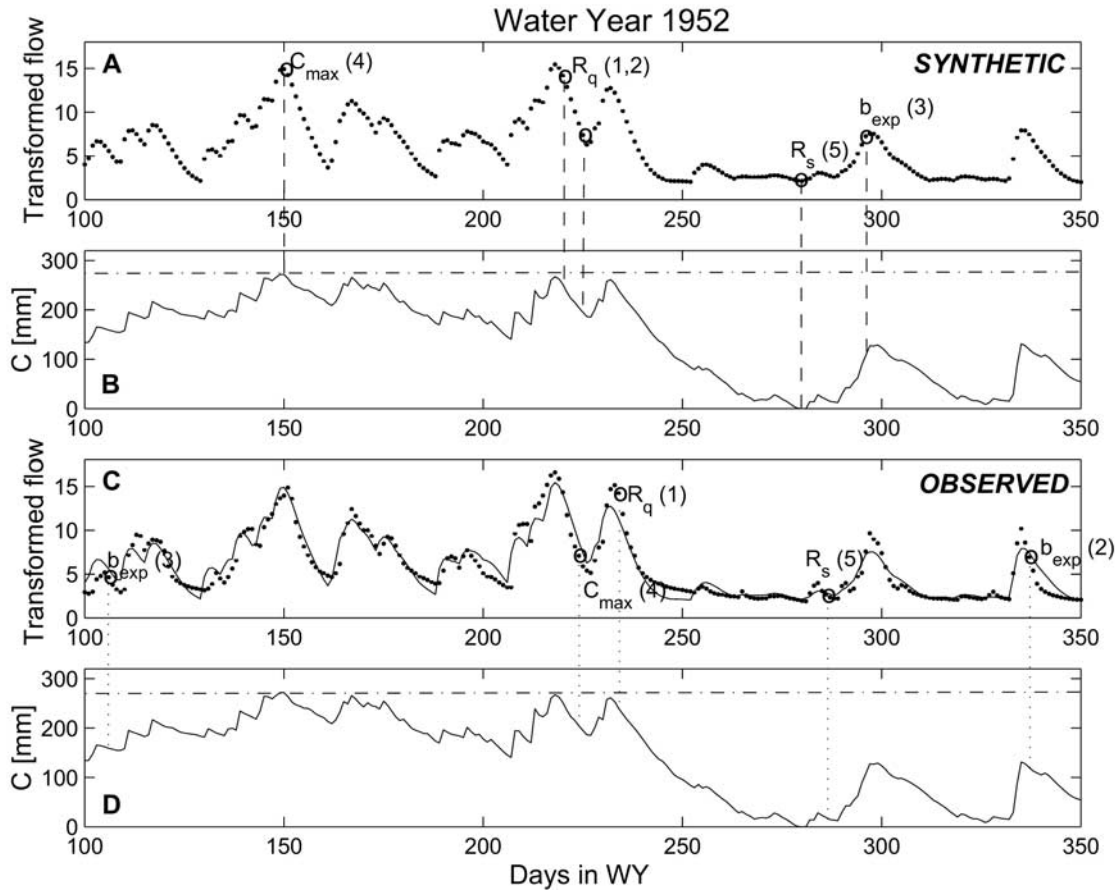
**Figure 8.** Location of the five most informative streamflow measurements along the hydrograph using synthetic (Figure 8a) and observed (Figure 8c) streamflow data (dots). The solid line in Figure 8c denotes the synthetic data. The hierarchical selection order of the measurements is indicated between parentheses. (b and d) Soil moisture storage dynamics derived using the "true" parameter set.

streamflow measurements for the parameter $C_{max}$ in the hydrograph is essentially dependent on the current state of the soil-moisture. When the conceptual soil compartment is saturated with water, then the identifiability of the $C_{max}$ parameter is at its maximum. Additionally, streamflows occurring at intermediate soil-moisture storages in the catchment contain the most information for the $b_{exp}$ parameter. Unfortunately, even after processing the five most informative measurements, no direct information was found for the parameter Alpha that partitions the streamflow into a quick and slow-flow component. Although not presented here, the HPD region converged readily into the vicinity of the true parameter values, after recursively assimilating and processing the 10 most informative streamflow measurements. The results for the observed streamflow data (HYMOD results indicated with solid line), presented in Figures 8c–8d demonstrate that there is a close correspondence in the location and hierarchical selection order of the HYMOD parameters found for the synthetic and observed streamflow measurements. The explicit presence of various sources of errors in the observed streamflows does not seem to significantly affect the location of the most informative streamflow measurement in the hydrograph for the various model parameters.

[38] Finally, in Figure 9 we present the evolution of the HPD region (light gray) and most likely parameter set (dark

line) as functions of the number of measurements processed using the PIMLI algorithm. The parameters were scaled according to their prior uncertainty ranges to yield normalized ranges. The asterisks correspond to the most likely parameter values derived using the SCE-UA global optimization algorithm. Without any calibration, the parameter ranges reflect their initial uncertainty, not conditioned on any input-output time series of measured streamflows. After processing the first 10 most informative streamflow measurements with the PIMLI algorithm, the HPD region narrows down rather quickly for most of the parameters. The characteristic jumping behavior of the HPD region throughout the feasible parameter space is caused by the presence of structural inadequacies in the HYMOD model and errors in the hydrological data. After recursively assimilating a sufficient amount of streamflow measurements with the PIMLI algorithm (40), the HPD region of the parameters finally settles down in the parameter space. The results in Figure 9 illustrate that the HYMOD model parameters are reasonably well determined by calibration to streamflow data. Note also the excellent correspondence between the most optimal parameter values identified using a conventional batch calibration approach (SCE-UA) for the entire 1-year period and the location of the HPD region derived with the PIMLI algorithm after processing only the 50 most informative streamflow measurements. It appears that the
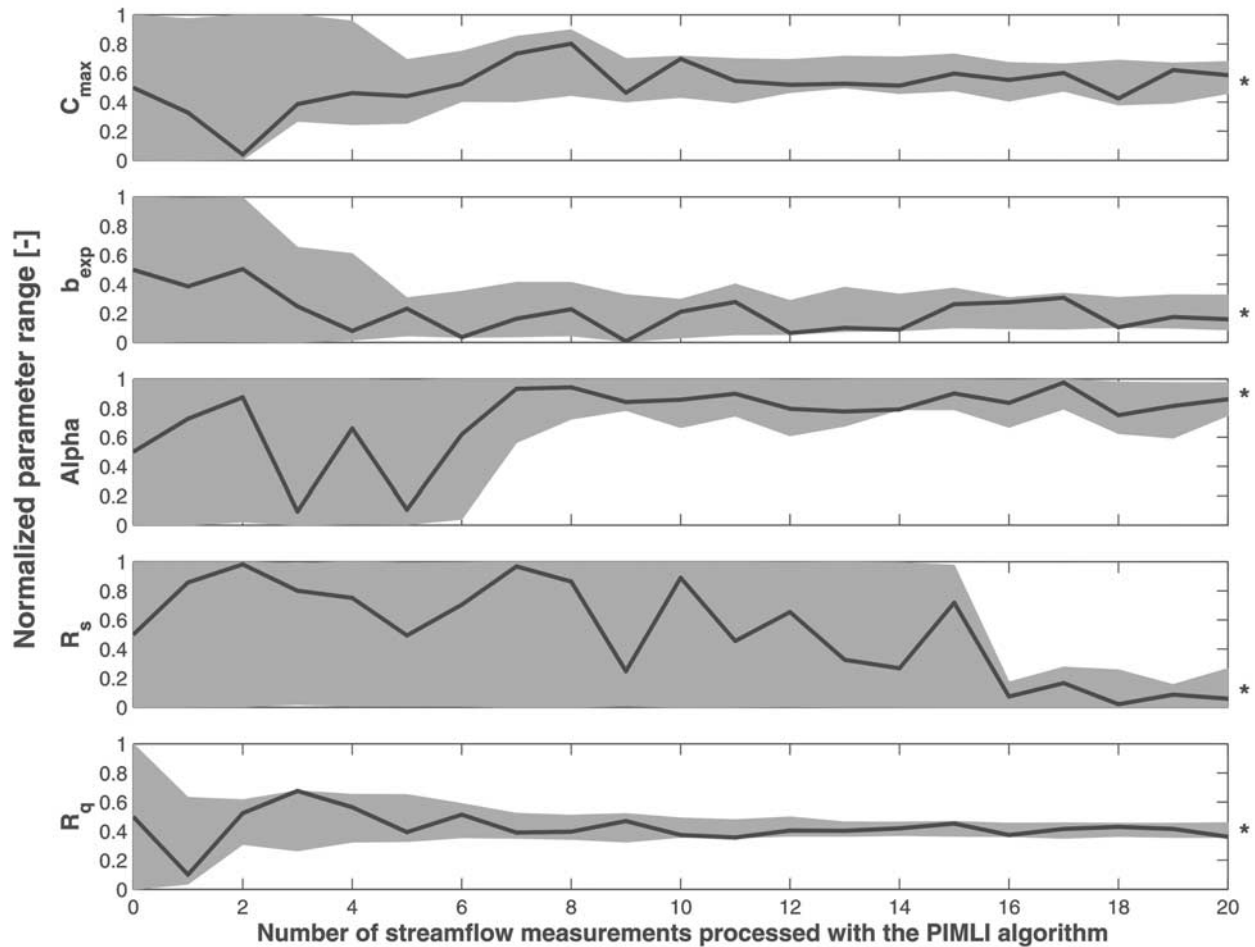
**Figure 9.**    Evolution of the 95% Bayesian confidence intervals (dotted lines) of the different parameters as a function of the number of streamflow measurements assimilated and processed using the PIMLI algorithm. The dashed lines indicate the most probable parameter values, whereas the asterisks denote the most likely parameter set derived when separately fitting the HYMOD model to the entire 1-year period of observed streamflow data using the SCE-UA algorithm.

use of disjunctive data regions that contain the highest information content for the parameters results in a reliable calibration of the HYMOD model, using only a very limited amount of streamflow measurements.

## 4.   Summary and Conclusions

[39] This paper has discussed a practical methodology entitled the PIMLI algorithm that merges the strengths of the Generalized Sensitivity Analyses, BARE algorithm, and Metropolis algorithm to identify sets of measurements that contain the most information for the identification of the model parameters. Three case studies with increasing complexity were used to illustrate the applicability and usefulness of the PIMLI methodology. The first two case studies considered estimating soil hydraulic parameters using soil water retention data and a more complex multistep transient outflow experiment. Finally, the third case study involved the calibration of a simple conceptual rainfall-runoff model using synthetic and observed streamflow data from the Leaf River watershed near Collins, Mississippi. The most obvious advantage of the PIMLI algorithm is that it infers

the type and location of the most informative measurements being associated with the different hydrologic parameters without having a priori knowledge of the system properties or most likely parameter set. The case study results suggest that the algorithm is well suited to identify which parameters control what part of model behavior, while providing insight into the importance of different kinds of data in experimental procedures. Finally, we believe that the PIMLI algorithm can be a valuable tool to help find complementary noncommensurable measures for multicriteria parameter estimation schemes, with each criterion being sensitive to a different parameter or aspect of model behavior.

# References

Beven, K. J., and A. M. Binley, The future of distributed models: Model calibration and uncertainty prediction, *Hydrol. Processes*, *6*, 279–298, 1992.

Box, G. E. P., and G. C. Tiao, *Bayesian Inference in Statistical Analyses*, Addison-Wesley-Longman, Reading, Mass., 1973.

Boyle, D. P., Multicriteria calibration of hydrological models, Ph.D. dissertation, Dep. of Hydrol. and Water Resour., Univ. of Ariz., Tucson, 2001.

Boyle, D. P., H. V. Gupta, and S. Sorooshian, Toward improved calibration of hydrological models: Combining the strengths of manual and automatic methods, *Water Resour. Res.*, *36*, 3663–3674, 2000.

Brazil, L. E., Multilevel calibration strategy for complex hydrological simulation models, Ph.D. dissertation, 217 pp., Colo. State Univ., Fort Collins, 1988.

Brazil, L. E., and W. F. Krajewski, Optimization of complex hydrologic models using random search methods, paper presented at Conference on Engineering Hydrology, Hydraulics Division, Am. Soc. of Civ. Eng., Williamsburg, Va., 3–7 Aug. 1987.

Brooks, R. H., and A. T. Corey, Hydraulic properties of porous media, *Hydrol. Pap., 3*, Civil Eng. Dep., Colo. State Univ., Fort Collins, 1964.

Duan, Q., V. K. Gupta, and S. Sorooshian, Effective and efficient global optimization for conceptual rainfall-runoff models, *Water Resour. Res.*, *28*, 1015–1031, 1992.

Duan, Q., V. K. Gupta, and S. Sorooshian, A shuffled complex evolution approach for effective and efficient global minimization, *J. Optim. Theory Appl.*, *76*(3), 501–521, 1993.

Duan, Q., S. Sorooshian, and V. K. Gupta, Optimal use of the SCE-UA global optimization method for calibrating watershed models, *J. Hydrol.*, *158*, 265–284, 1994.

Duan, Q., J. Schaake, and V. Koren, A priori estimation of land surface model parameters, in *Land Surface Hydrology, Meteorology and Climate, Water Sci. Appl.*, vol. 3, edited by V. Lakshmi, J. Albertson, and J. Schaake, pp. 77–94, AGU, Washington, D. C., 2001.

Freer, J., K. J. Beven, and B. Ambroise, Bayesian estimation of uncertainty in runoff prediction and the value of data: An application of the GLUE approach, *Water Resour. Res.*, *32*, 2161–2173, 1996.

Gelman, A., and D. B. Rubin, A single series from the Gibbs sampler provides a false sense of security, in *Bayesian Statistics 4*, edited by J. M. Bernardo et al., pp. 625–632, Oxford Univ. Press, New York, 1992.

Gelman, A., J. B. Carlin, H. S. Stren, and D. B. Rubin, *Bayesian Data Analysis*, Chapman and Hall, New York, 1997.

Gupta, H. V., S. Sorooshian, and P. O. Yapo, Toward improved calibration of hydrologic models: Multiple and non-commensurable measures of information, *Water Resour. Res.*, *34*, 751–763, 1998.

Gupta, V. K., and S. Sorooshian, The relationship between data and the precision of parameter estimates of hydrological models, *J. Hydrol.*, *81*, 57–77, 1985.

Hollenbeck, K. J., and K. H. Jensen, Maximum-likelihood estimation of unsaturated hydraulic parameters, *J. Hydrol.*, *210*, 192–205, 1998.

Janssen, P. H. M., and P. S. C. Heuberger, Calibration of process-oriented models, *Ecol. Model.*, *83*, 55–66, 1995.

Keesman, K. J., Set theoretic parameter estimation using random scanning and principal component analysis, *Math. Comput. Simul.*, *32*, 535–543, 1990.

Kirkpatrick, S., C. D. Gellat, and M. P. Vecchi, Optimization by simulated annealing, *Science*, *220*, 671–680, 1983.

Klepper, O., H. Scholten, and J. P. G. van de Kamer, Prediction uncertainty in an ecological model of the Oosterschelde Estuary, *J. Forecasting*, *10*, 191–209, 1991.

Kool, J. B., and J. C. Parker, Analysis of the inverse problem for transient unsaturated flow, *Water Resour. Res.*, *24*, 817–830, 1988.

Kosugi, K., Lognormal distribution model for unsaturated soil hydraulic properties, *Water Resour. Res.*, *32*, 2697–2703, 1996.

Kuczera, G., On the relationship of the reliability of the parameter estimates and hydrological time series data used in calibration, *Water Resour. Res.*, *18*, 146–154, 1982.

Kuczera, G., On validity of first-order prediction limits for conceptual hydrological models, *J. Hydrol.*, *103*, 229–247, 1988.

Kuczera, G., and E. Parent, Monte Carlo assessment of parameter uncertainty in conceptual catchment models: The Metropolis algorithm, *J. Hydrol.*, *211*, 69–85, 1998.

Luckner, L., M. T. van Genuchten, and D. R. Nielsen, A consistent set of parametric models for the 2-phase flow of immiscible fluids in the subsurface, *Water Resour. Res.*, *25*, 2187–2193, 1989.

Metropolis, N., A. W. Rosenbluth, M. N. Rosenbluth, A. H. Teller, and E. Teller, Equations of state calculations by fast computing machines, *J. Chem. Phys.*, *21*, 1087–1091, 1953.

Moore, R. J., The probability-distributed principle and runoff production at point and basin scales, *Hydrol. Sci. J.*, *30*(2), 273–297, 1985.

Mualem, Y., A new model for predicting the hydraulic conductivity of unsaturated porous media, *Water Resour. Res.*, *12*, 513–522, 1976.

Parker, J. C., J. B. Kool, and M. T. van Genuchten, Determining soil hydraulic properties from one-step outflow experiments by parameter estimation, II, Experimental studies, *Soil Sci. Soc. Am. J.*, *49*, 1354–1359, 1985.

Rossi, C., and J. R. Nimmo, Modeling of soil water retention from saturation to oven dryness, *Water Resour. Res.*, *30*, 701–708, 1994.

Russo, D., Determining soil hydraulic properties by parameter estimation: On the selection of a model for the hydraulic properties, *Water Resour. Res.*, *24*, 453–459, 1988.

Schaap, M. G., F. J. Leij, and M. T. van Genuchten, Neural network analysis for hierarchical prediction of soil hydraulic properties, *Soil Sci. Soc. Am. J.*, *62*, 847–855, 1998.

Šimůnek, J., M. Šejna, and M. T. van Genuchten, The HYDRUS-1D software package for simulating the one-dimensional movement of water, heat, and multiple solutes in variably-saturated media, version 2.0, 202 pp., *Rep. IGWMC-TPS-70*, Int. Ground Water Model. Cent., Colo. Sch. of Mines, Golden, 1998a.

Šimůnek, J., O. Wendroth, and M. T. van Genuchten, Parameter estimation analysis of the evaporation method for determining soil hydraulic properties, *Soil Sci. Soc. Am. J.*, *62*, 894–905, 1998b.

Sorooshian, S., and J. A. Dracup, Stochastic parameter estimation procedures for hydrological rainfall-runoff models: Correlated and heteroscedastic error cases, *Water Resour. Res.*, *16*, 430–442, 1980.

Sorooshian, S., V. K. Gupta, and J. L. Fulton, Evaluation of maximum likelihood parameter estimation techniques for conceptual rainfall-runoff models: Influence of calibration data variability and length on model credibility, *Water Resour. Res.*, *19*, 251–259, 1983.

Sorooshian, S., Q. Duan, and V. K. Gupta, Calibration of rainfall-runoff models: Application of global optimization to the Sacramento soil moisture accounting model, *Water Resour. Res.*, *29*, 1185–1194, 1993.

Spear, R. C., and G. M. Hornberger, Eutrophication in the Peel Inlet, II, Identification of critical uncertainties via generalized sensitivity analysis, *Water Res.*, *14*, 43–49, 1980.

Spear, R. C., T. M. Grieb, and N. Shang, Parameter uncertainty and interaction in complex environmental models, *Water Resour. Res.*, *30*, 3159–3169, 1994.

Thiemann, M., M. Trosset, H. Gupta, and S. Sorooshian, Bayesian recursive parameter estimation for hydrological models, *Water Resour. Res.*, *37*, 2521–2535, 2001.

van Genuchten, M. T., A closed-form equation for predicting the hydraulic conductivity of unsaturated soils, *Soil Sci. Soc. Am. J.*, *44*, 892–898, 1980.

van Straten, G., and K. J. Keesman, Uncertainty propagation and speculation in projective forecasts of environmental change: A lake eutrophication example, *J. Forecasting*, *10*, 163–190, 1991.

Vereecken, H., R. Kaiser, M. Dust, and T. Pütz, Evaluation of the multi-step outflow method for the determination of unsaturated hydraulic properties of soil, *Soil Sci.*, *162*, 618–631, 1997.

Vrugt, J. A., and W. Bouten, Validity of first order approximations for assessing parameter uncertainty in soil hydrological models, *Soil Sci. Soc. Am. J.*, in press, 2002.

Vrugt, J. A., A. H. Weerts, and W. Bouten, Information content of data for identifying soil hydraulic parameters from outflow experiments, *Soil Sci. Soc. Am. J.*, *65*(1), 9–27, 2001.

Wagener, T., D. P. Boyle, M. J. Lees, H. S. Wheater, H. V. Gupta, and S. Sorooshian, A framework for development and application of hydrological models, *Hydrol. Earth Syst. Sci.*, *5*(1), 13–26, 2001.

Wang, Q. J., The genetic algorithm and its application to calibrating conceptual rainfall-runoff models, *Water Resour. Res.*, *27*, 2467–2471, 1991.

——————————
W. Bouten and J. A. Vrugt, Institute for Biodiversity and Ecosystem Dynamics, University of Amsterdam, Nieuwe Achtergracht 166, Amsterdam 1018 WV, Netherlands. (j.vrugt@science.uva.nl)

H. V. Gupta and S. Sorooshian, Department of Hydrology and Water Resources, University of Arizona, Tucson, AZ 85721, USA.